Wear Characteristics and Cleaning Ability of Cleaning Blades

Kuniki Seino▲ and Shizuo Yuge
Toyokawa Development Center, Minolta Co. Ltd., Toyokawa, Aichi, Japan

Masao Uemura
Toyohashi University of Technology, Toyohashi, Aichi, Japan

The cleaning performance (lifetime of cleaning blades and cleaning ability) of a leading type blade cleaning system for electrophotography is examined theoretically and experimentally from the viewpoint of tribology and rheology. Wear characteristics and cleaning ability of cleaning blades are found to be described well by a model which takes into account stick–slip behavior of the cleaning blade against a photoreceptor surface. A theoretical analysis of fatigue wear which takes into account vibration loss tangent (or rebound resilience), applied load on the cleaning blade on the photoreceptor surface, and friction coefficient between the blade edge and the photoreceptor surface, agrees well with results of accelerated wear experiments and lifetime evaluation tests using copying machines on the market. The cleaning blade edge once stretched by the photoreceptor surface during the stick process returns to its original position gradually with a characteristic relaxation time during the slip process and forces remaining toner particles to move against the rotating direction of photoreceptor drum. Therefore, toner particles have a greater possibility of going through the blade nip during the slip process. The theoretical analysis and the experimental results suggest that cleaning ability is proportional to the reciprocal of the relaxation time.

Journal of Imaging Science and Technology 47: 424-433 (2003)

Introduction

A blade cleaning method is widely used in electrophotographic copying machines and printers. However, there is still a strong demand for better cleaning ability and longer lifetime of cleaning blade.[1] Toners have been made increasingly fine in diameter and maintenance-free engines are of urgent necessity. We have previously reported that in a leading type blade cleaning system the cleaning performance (lifetime of cleaning blades and cleaning ability) strongly depends on the rebound resilience (R) of the polyurethane rubber.[2] However, there have been few reports that investigated systematically the relationship between the rebound resilience and the cleaning performance. A large number of research works on general wear of rubber have been reported.[3,4] However, there have been few reports on the wear mechanism of the cleaning blade for electrophotography. In this article, we examine the cleaning performance of the leading type blade cleaning system theoretically and experimentally from the viewpoint of tribology and rheology.

Original manuscript received January 23, 2003

▲ IS&T Senior Member

©2003, IS&T—The Society for Imaging Science and Technology

Wear Characteristics of Cleaning Blade

Mechanism of Wear

Figure 1 gives a conceptual view of our leading type blade cleaning system for electrophotography. The cleaning blade is pressed on a photoreceptor drum by spring tension. A magnified conceptual view of the neighborhood of the blade edge is also illustrated in Fig. 1. Untransferred toner particles are blocked by the cleaning blade and accumulate to form a pool of toner. The blade nip is reported to be several tens of microns.[5]

Figure 2 gives a conceptual view of stick–slip behavior of a cleaning blade. When a cleaning blade sticks on a photoreceptor surface, it is stretched in the direction towards which the photoreceptor layer moves (Figs. 2(a) and 2(b)). Repulsive force on the cleaning blade increases in proportion to the stretched length of the blade edge. The stretch can be illustrated using the Voigt Model, such that one side is stretched by frictional force in the direction towards which the photoreceptor layer moves while the other side is fixed (Figs. 2(d) and 2(e)). When the repulsive force reaches the static friction force between the blade nip and the photoreceptor surface, the blade edge begins sliding and returns towards its original position, because the coefficient of kinetic friction is smaller than that of static one (Figs. 2(b) and 2(c)). As the blade edge approaches the original position, its repulsive force decays. Then, as soon as the repulsive force equals the kinetic friction force (Fig. 2(d)), the blade nip sticks again on the photoreceptor surface. The repeated cycles of stick–slip motion force the blade edge to be worn out by fatigue, stripping off small fragments of polyurethane rubber in the process.

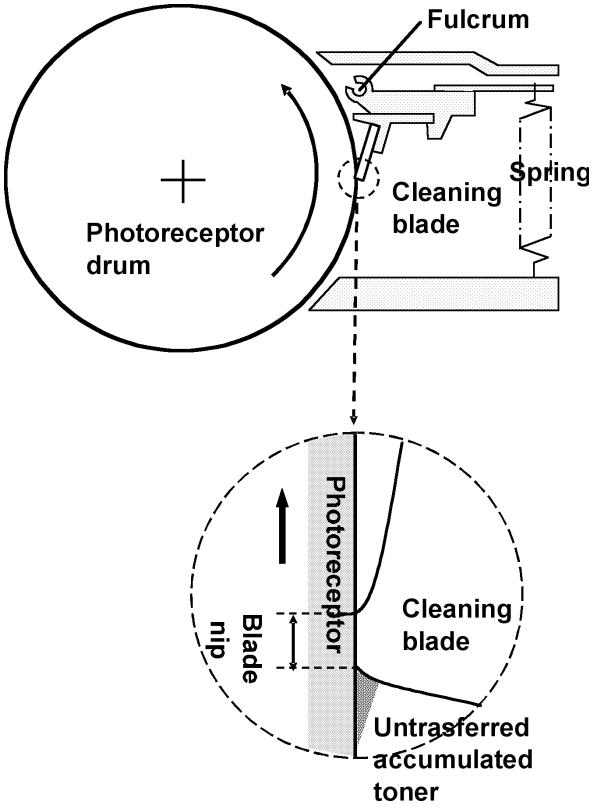

Figure 1. A conceptural view of a leading-type blade cleaning system and the vicinity of the blade edge.

Figure 3 shows SEM photographs of a worn surface of the worn cleaning blade edges. The worn surface has microscopic roughness showing alternating ridges and grooves. This pattern is generated by friction against a relatively smooth surface, and suggests that the blade edge is destroyed by fatigue destruction.

We consider a wear model where small worn fragments of the cleaning blade (denoted as "worn particles") are stripped off one by one, caused by fatigue destruction as shown in Fig. 4. A newly generated crack **p→q** after stripping off the worn particle and a crack growth process **p→q→r→s** are indicated in Fig. 4(a). When very small applied load is added to the cleaning blade in Fig. 4(b), an area BC and a point A contact with the photoreceptor surface. When the maximum applied load acts on the blade nip in Fig. 4(c), nearly all of the worn surface contacts the photoreceptor surface and is stretched in the direction towards which the photoreceptor layer moves. Expected pressure distribution acting on the contact area is also illustrated in Fig. 4(c). As the photoreceptor continues to rotate, the repulsive force of the blade edge approaches the static friction force between the blade edge and the photoreceptor surface. Then, in the neighborhood of point B, between A and B where the pressure is lower, the blade slides locally by a kind of Mindlin slip[6] as shown in Fig. 4(d). When this area slides, other contact area between A and B cannot bear the repulsive force of the blade edge. Consequently the whole area between A and B slides and the stretch force acts to cause a crack **p→q** shown in Fig. 4(d). Finally the crack tears and the small crack **p→q** grows towards the direction bisecting the angle **p'q p"** in Fig. 4(e), and

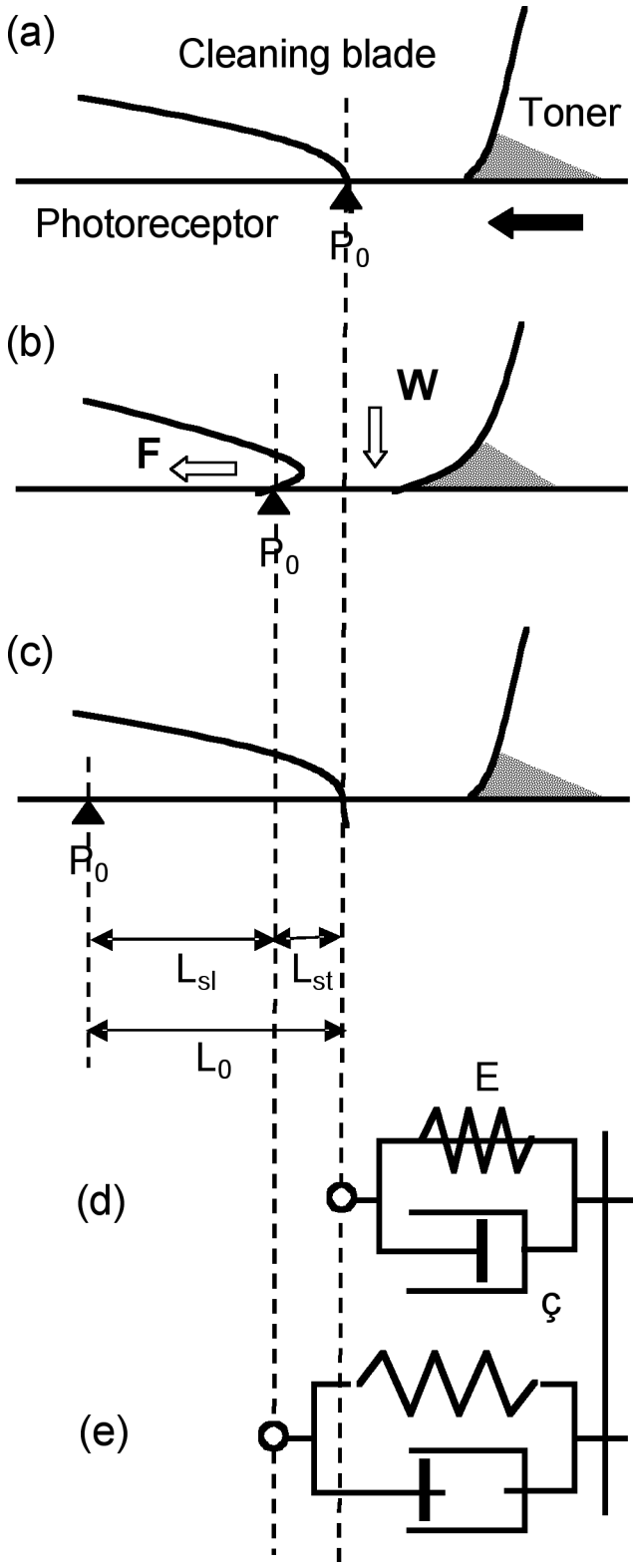

Figure 2. A stick-slip cycle governed by viscoelastic properties of cleaning blades and the Voigt model. W and F indicate weight on the photoreceptor surface and friction force for the cleaning blade respectively (a) – (b): stick process. Position P_0 on the photoreceptor surface moves by L_{st} (b) – (c): slip process. Position P_0 moves by L_{sl} while the cleaning blade edge returns to the original position with a relaxation time during slip motion. L_0: friction length per one cycle of the stick-slip. L_{st}: stick length. L_{sl}: slip length.

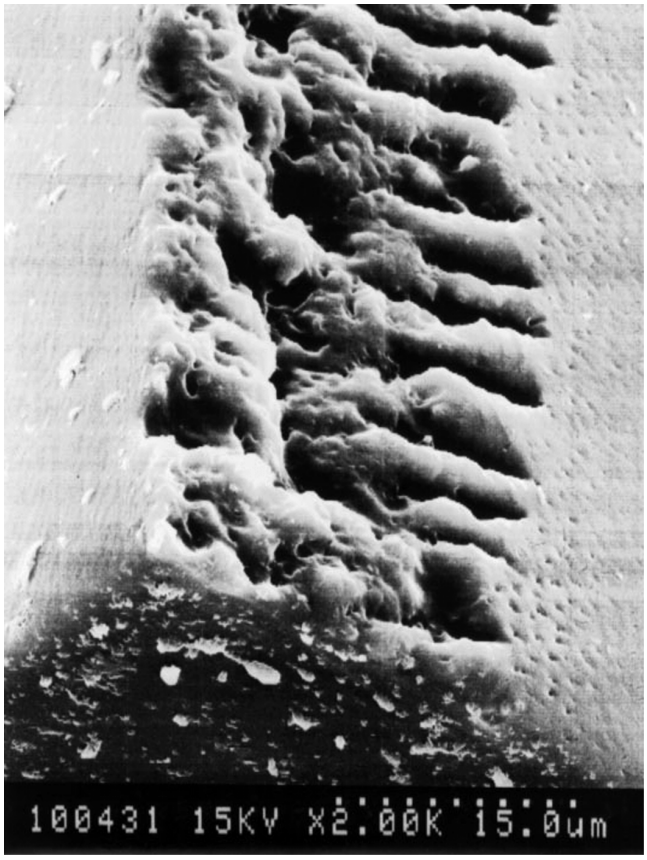

Figure 3. SEM photographs of a surface of the worn cleaning blade edges.

the whole nip area slides. According to crack geometry **p'q** is larger than **p"q**, therefore, the crack grows tracing a circular arc **p**→**q**→**r**→**s** shown in Fig. 4(a).

Consider a cleaning blade with a worn surface of width z as shown in Fig. 5. For simplicity, it is assumed that worn particles are cubes of $a \times b \times c$. By stripping off the particles one by one from the right side (the front to the rear of the blade) along the z direction, grooves with a width of c and an average thickness of $b/2$ are formed. When the width z is worn out, the number of total worn particles generated is z/a. Denoting the number of friction vibrations required for generating one worn particle by N_0, and the friction length per one cycle of the stick–slip by L_0, the unit friction length L_u necessary to wear out one layer of particle thickness can be expressed as follows:

$$L_u = N_0 L_0 \, z/a \tag{1}$$

Because the average worn height of the groove is $b/2$, the worn height per unit friction length is given by,

$$(b/2)/L_u = ab/2N_0L_0 \, z \tag{2}$$

Based on Eq. (2), an infinitely small worn height Δh for an infinitely small sliding length Δl can be expressed as,

$$\Delta h/\Delta l = ab/2N_0L_0 z = ab\sin\theta \cos\theta /2N_0L_0h \tag{3}$$

where the angle θ is defined in Fig. 5. Then, in the limit

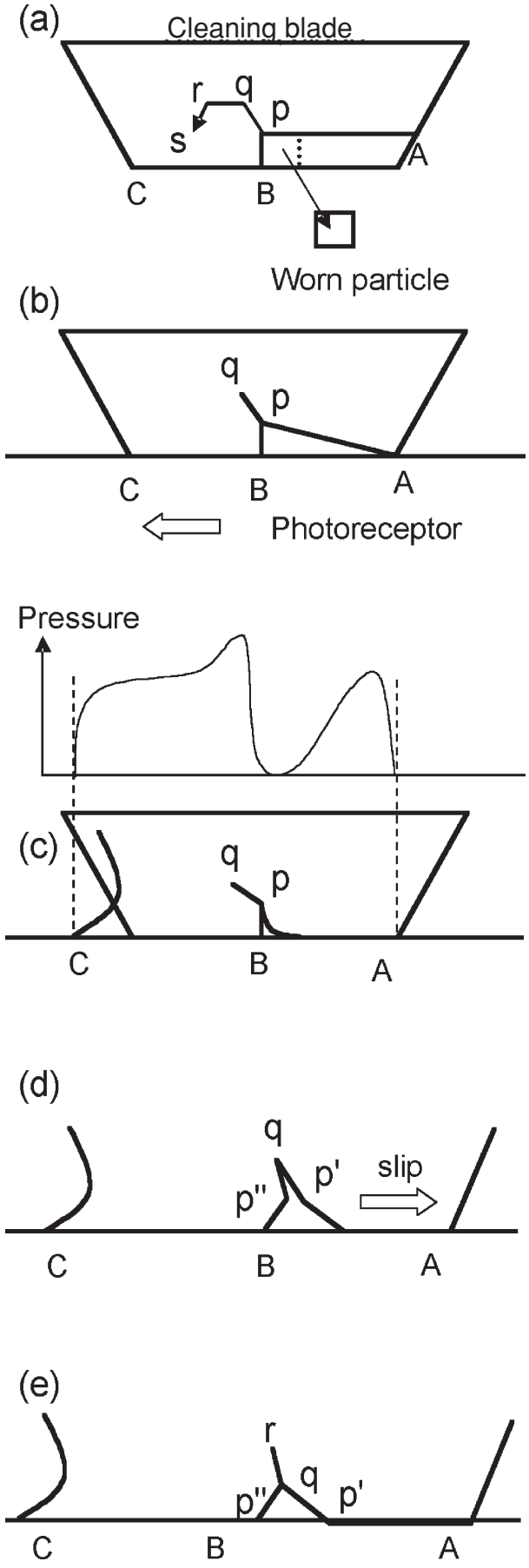

Figure 4. Mechanism of generating worn particles.

TABLE I. Blade Characteristics

Sample No.		Rebound Resiliences 20°C	25°C	30°C	Hardness (JIS A)	Shearing Strss (Kg/cm)	300% modulus (Kg/cm²)	Young's modulus (Kg/cm²)
1	×	27	37	45	69	67	110	63
2	✳	27	37	46	68	37	140	69
3	□	39	50	57	77	73	147	87
4	○	51	59	64	79	81	105	84
5	△	58	65	71	69	48	100	59
6	◊	66	71	74	70	57	73	60
7	✢	64	71	76	64	43	75	57
8		41	54	61	67	52	130	55

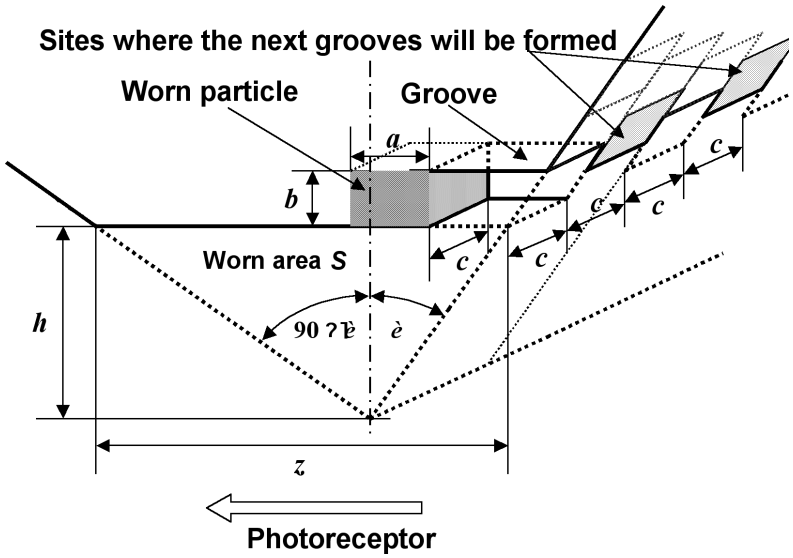

Figure 5. Geometry of worn blade edge, showing the formation of worn particles with dimension $a \times b \times c$, in the worn surface.

where Δl approaches 0,

$$dh/dl = \alpha \sin\theta \cos\theta/h \quad (4)$$

$$\alpha = ab/2N_0 L_0 \quad (5)$$

Friction Coefficient of Cleaning Blade

The experimental arrangement for measuring friction force and contact area between the cleaning blade edge and the photoreceptor surface is shown in Fig. 6. An organic photoreceptor drum with a diameter of 100 mm was used. Cleaning blades were pressed onto the photoreceptor surfaces with a micrometer and the applied load was measured by a load cell. The contact angle was 18°. The cleaning blades made of thermohardened polyurethane rubber were studied. Blade characteristics are listed in Table I.

The sample No. 8 in Table I was tested. The length of test pieces of polyurethane blades was 60 mm, the width 15 mm, and the thickness 2 mm. The friction force was measured by a torque meter connected to the photoreceptor drum axis. The measured quantity is the average of static and kinetic friction coefficients, because both stick and slip behavior influence.

The contact area is observed by replacing the photoreceptor drum with a transparent glass cylinder of the same diameter containing a CCD camera inside. The following empirical relationship between the apparent contact area A_n and the applied load W is obtained from the experimental result shown in Fig. 7.

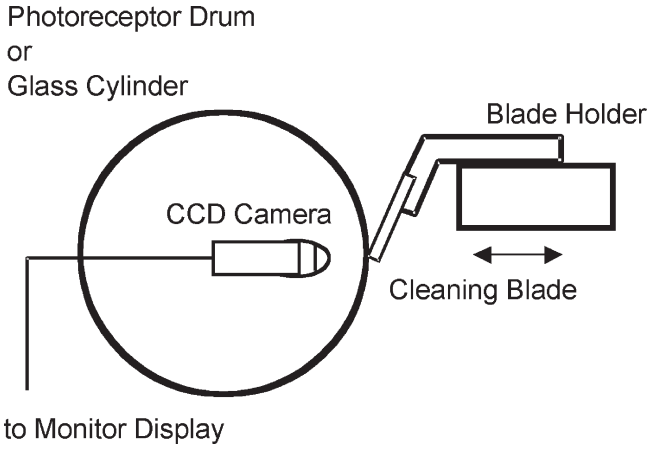

Figure 6. Experimental arrangement of laboratory tester for friction and apparent contact area.

$$A_n = 42.4W^{0.50} \quad (6)$$

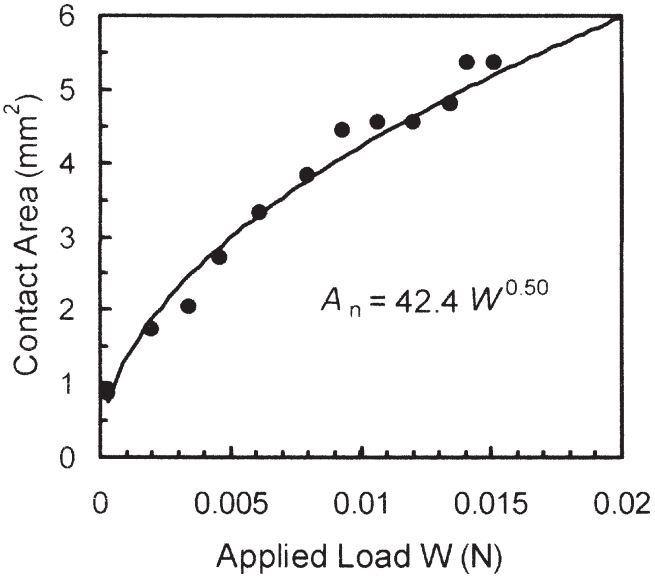

Figure 7. Typical example of relationship between the apparent contact area and the weight for polyurethane cleaning blade. The solid curve is calculated from Eq. (6).

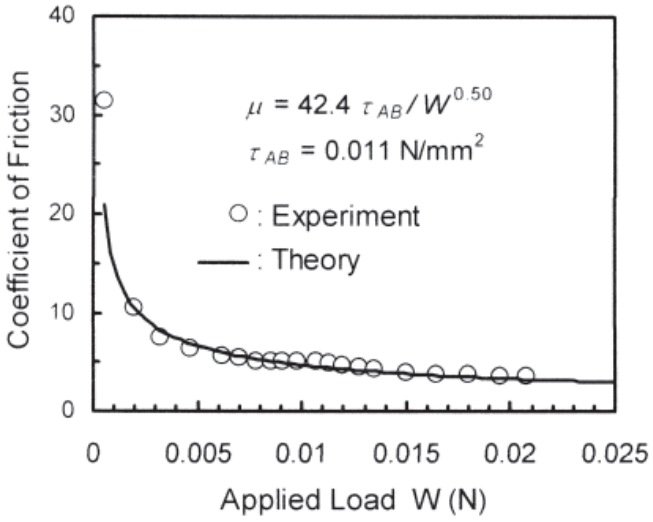

Figure 8. Typical example of relationship between coefficient of friction and weight for polyurethane blade at the photoreceptor surface. The solid curve is calculated from Eq. (8) with $\tau_{AB} = 0.012\ N/mm^2$.

The case where a corner edge of the cleaning blade is pressed onto the photoreceptor surface corresponds to a contact between a single protrusion and a plane. Under the assumption that the apparent contact area A_n is equal to the real contact area A_r, the friction force is given by

$$F = \tau_{AB} A_n \tag{7}$$

where τ_{AB} is the average shear strength. The substitution of Eq. (7) into Eq. (6) yields the coefficient of friction μ as,

$$\mu = F/W = 42.4\tau_{AB}/W^{0.50} \tag{8}$$

The results of the friction coefficient measurements are shown in Fig. 8. Good agreement with the curve calculated with $\tau_{AB} = 0.011$ N/mm^2 using Eq. (8) indicates that shear strength is constant regardless of applied load and pressure.

Frictional Vibrations

The laboratory test regarding fatigue was carried out in order to investigate the mechanism of fatigue wear. The thermohardened polyurethane rubber was studied. A fatigue tester and a shape of test pieces are shown in Figs. 9 and 10, respectively. The sample No. 8 in Table I was tested at 25°C and 50°C. The fatigue test was carried out with average stress = maximum stress/2. The speed of repeating stress cycles was 1 Hz and the amplitudes of strain were 2, 4, 6, 8 and 10 cm. The fatigue destruction is defined as a phenomenon that under repeated cycles of stress a material is destroyed with less than the destruction stress. The number of repeated cycles N_c to destruction is called the repeated cycles to life. Based on the experimental results shown in Fig. 11, the reciprocal of repeated cycles to life N_c is found to relate to the stress s as,

$$1/N_c \propto \sigma^m \tag{9}$$

where $m = 6.5$ at 25°C and $m = 7.0$ at 50°C.

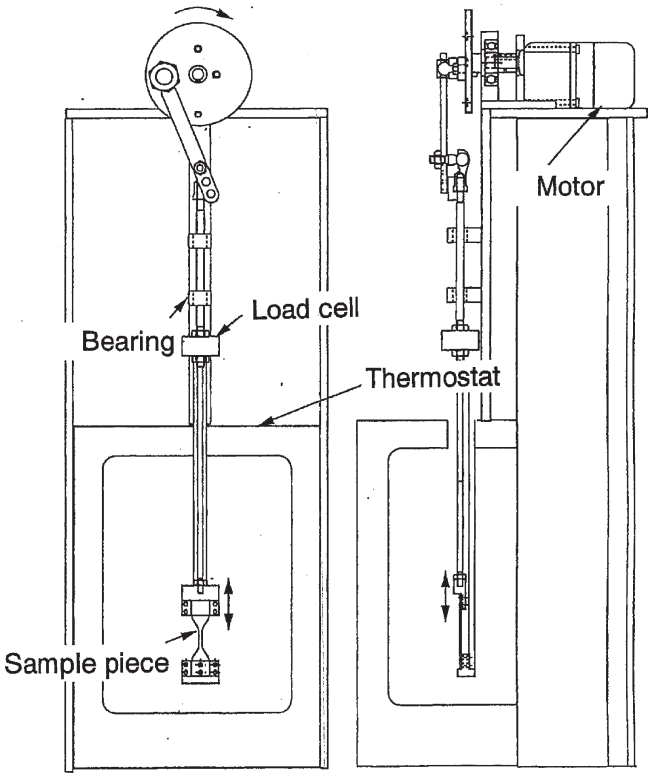

Figure 9. Schematic diagram of fatigue tester.

According to the mechanism of wear shown in Fig. 4, when the area BC sticks and the area AB slips completely, the maximum force acts to the area BC as shown in Fig. 4(d). Because this maximum force is considered to be nearly equal to the static friction force that acts on the area BC, the maximum stress that acts on the area BC is nearly equal to the maximum shear strength

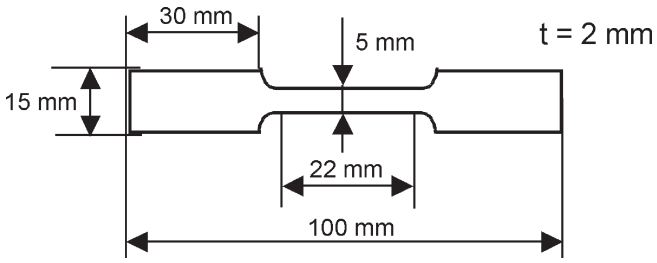

Figure 10. Sample piece for fatigue tester.

which acts to the contact interface. It is generally considered that the ratio of static to kinetic friction forces is constant in the case of normal friction. Therefore the maximum force that acts on the area BC is proportional to the shear strength τ_{AB} determined in Fig. 8. Then, the number of repeated cycles to destruction N_c and the stress σ in Eq. (9) are considered to be proportional to the number of frictional vibrations for generating one worn particle, N_0, and the average shear strength, τ_{AB}, respectively. Therefore, Eq. (9) can be rewritten as

$$1/N_c \propto 1/N_0 \propto \sigma^m \propto {\tau_{AB}}^m \tag{10}$$

Microscopic roughness develops on the wear surface of the cleaning blade (see Fig. 3). When microscopic convex points contact the photoreceptor surface, there might be a possibility that the shear strength at the worn contact area is not equal to the shear strength τ_{AB} measured for cleaning blades without wear. However, if we assume that τ_{AB} is constant regardless of the applied load, the coefficient of friction is adequately explained over a wide range. This implies that τ_{AB} is constant regardless of the wear of cleaning blades. Therefore, the following equation is obtained by substituting τ_{AB} from Eq. (8) into Eq. (10),

$$N_0 \propto {\tau_{AB}}^{-m} \propto (\mu\ W^{0.50})^{-m} \tag{11}$$

where μ is the coefficient of friction measured for cleaning blades without wear.

Friction Length

As shown in Fig. 2(c) a point P_0 on the photoreceptor surface moves by L_{st} during the stick process and L_{sl} during the slip process; then the friction length per one cycle of the stick–slip, L_0, is given by:

$$L_0 = L_{st} + L_{sl} \tag{12}$$

where L_{st} is the stick length and L_{sl} is the slip length.

We apply the Voigt model shown in Fig. 2(d) and 2(e) to the stick–slip behavior of cleaning blades, where E is the elasticity and η is the viscosity. During the stick process (Figs. 2(d) and 2(e)) the repulsive force of the blade edge increases in proportion to stretched length γ. When the repulsive force reaches the static friction force F_s, relative sliding results between the photoreceptor surface and the blade nip. Assuming $\gamma = \gamma_0$ at this point, we have,

$$F_s = E\gamma_0 = \mu_s W \tag{13}$$

where μ_s is the coefficient of static friction.

The cleaning blade nip returns to its original position gradually with a relaxation time during the slip process (Figs. 2(e) and 2(d)), and the length γ during the slip process can be expressed by the following equations:

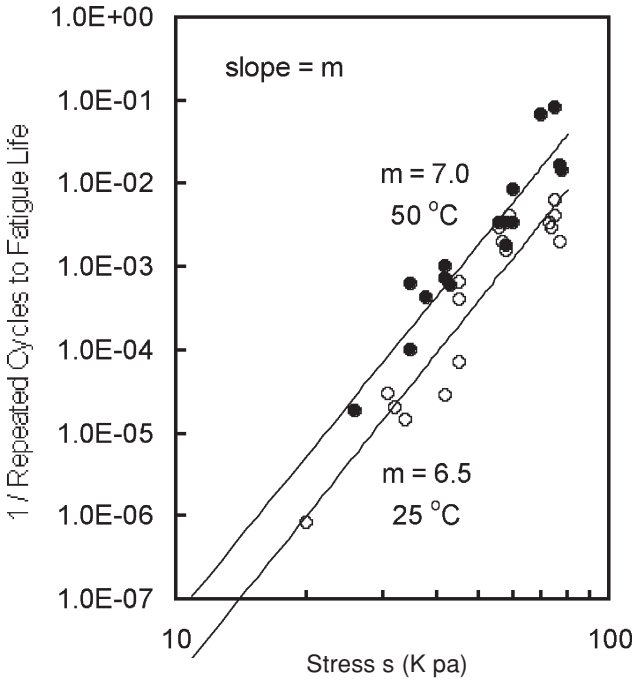

Figure 11. The reciprocal of repeated cycles to life as a function of stress to polyurethane rubber.

$$F_k = E\gamma + \eta\, d\gamma/dt \tag{14}$$

where F_k is the kinetic friction force. The general solution of Eq. (14) is given by

$$\gamma = F_k/E + C\exp(-t/\tau) \tag{15}$$

where τ (= η/E) is the relaxation time. The length γ contracts until the repulsive force equals the kinetic friction force F_k. Denoting γ at this point as γ_k, we have,

$$F_k = E\gamma_k = \mu_k W \tag{16}$$

where μ_k is the coefficient of kinetic friction. Assuming Eq. (13) applies at $t = 0$ and that Eq. (16) applies at $t = \infty$, we obtain that Eq. (15) leads to Eqs. (17) and (18).

$$\gamma = \gamma_k + (\gamma_0 - \gamma_k)\exp(-t/\tau) \tag{17}$$

$$t = \tau \ln\{(\gamma_0 - \gamma_k)/(\gamma - \gamma_k)\} \tag{18}$$

When the repulsive force decays relative to any friction force, the cleaning blade nip sticks on the photoreceptor surface. However it takes infinite time until γ reaches γ_k as indicated by Eq. (18). In the case of our leading type blade cleaning system the cleaning blade is pressed on a photoreceptor surface by spring tension as shown in Fig. 1. Therefore, the blade edge is stretched upward in Fig. 1 and the cleaning blade is in close contact with the photoreceptor surface. As the blade edge approaches the photoreceptor surface, the spring shrinks due to geometrical arrangement of the fulcrum shown in Fig. 1, and then the applied load acting on the cleaning blade decreases. Contrary to this, as the blade edge re-

turns to the original position, the applied load increases, and then the kinetic friction force increases. The kinetic friction force increases with increasing applied load; however, in order to simplify the equations, we assume that the kinetic friction force increases with increasing kinetic friction coefficient keeping the applied load constant. Expressing the incremental friction force with the incremental friction coefficient $\delta\mu$, and assuming that the blade nip sticks on the photoreceptor surface again when γ decays to $\gamma_k + \delta\mu\ W/E$, the substitution of Eq. (13) and Eq. (16) into Eq. (18) yields the slip time t_{sl+}as

$$t_{sl} = \tau \ln\{(\mu_s - \mu_k)/\delta\mu\} \tag{19}$$

Therefore, the slip length L_{sl} can be given by

$$L_{sl} = vt_{sl} = v\tau \ln\{(\mu_s - \mu_k)/\delta\mu\} \tag{20}$$

where v is the rotating velocity of the photoreceptor drum. Then the stick length L_{st} can be expressed as follows:

$$L_{st} = \gamma_0 - (\gamma_k + \delta\mu W/E) = (\mu_s - \mu_k - \delta\mu)W/E \tag{21}$$

The substitution of Eq. (20) and (21) into Eq. (12) yields the friction length per one cycle of the stick–slip L_0 as

$$L_0 = (\mu_s - \mu_k - \delta\mu)\ W/E + v\tau \ln\{(\mu_s - \mu_k)/\delta\mu\} \tag{22}$$

In the case of the Voigt model, the following relationship is well known

$$\tan\delta = \omega\tau \tag{23}$$

However, rebound resilience R is widely used rather than vibration loss, tan δ, as a method for measuring viscoelastic properties of cleaning blades. The relationship between rebound resilience (expressed in decimal form) and tan δ are related by[7]

$$R = \exp(-\pi \tan\delta) \tag{24}$$

We obtain the friction length per one cycle of the stick–slip L_0 in the following form by substituting Eqs. (23) and (24) into Eq. (22):

$$L_0 = (\mu_s - \mu_k - \delta\mu)\ W/E - (v/\omega\pi) \ln\{(\mu_s - \mu_k)/\delta\mu\} \ln R \tag{25}$$

Both the coefficients of static and kinetic friction might change with wear of blade edges. However, because the kinetic friction force increases with the static friction force, $(\mu_s - \mu_k)$ is considered not to depend strongly on the wear of the blade edges. Furthermore, the change of $\delta\mu$ due to the wear can be neglected because the wear volume is much less than the compressed volume at the blade nip.

Wear Equation

The cross-sectional area S of worn cleaning blade edges shown in Fig. 5 is expressed as follows:

$$S = zh/2 = h^2/2\sin\theta\cos\theta \tag{26}$$

Differentiating and using Eq. (4), we obtain to the following equation:

$$dS = h\ dh/\sin\theta\cos\theta = \alpha\ dl \tag{27}$$

Then the cross-sectional area is given by

$$S = \alpha\ l \tag{28}$$

Substituting Eq. (11) and (25) into Eq. (5), the wear speed is given by

$$\alpha = C'\mu^m W^{0.5m} \left\{\frac{(\mu_s - \mu_k - \delta\mu)W}{E} - \left(\frac{\nu}{\varpi\pi}\right)\ln\left(\frac{\mu_s - \mu_k}{\delta\mu}\right)\ln R\right\}^{-1} \tag{29}$$

Experimental

The cleaning blades made of thermohardened polyurethane rubber were studied. The specifications of the cleaning blades used are shown in Table I. The rebound resilience R was measured by using a Lüpke type testing apparatus. The rebound resilience is defined as the ratio of the energy after rebound to that before rebound when a pendulum having a spherical collision surface impacts a test sample. The rebound resilience of polyurethane strongly depends on temperature as shown in Table I.

A 60 copies per minute copying machine was used as an experimental apparatus. The photoconductive drum was kept at 30°C with a heater. The development method was the Micro-Toning system, and the toner was styrene-acrylic resin based toner with the average diameter of 11 μm.

A schematic diagram of the blade cleaning system used for experiment is shown in Fig. 1. The main cleaning specifications were as follows:

- Cleaning method: Leading type
- Length of blade: 338 mm
- Free length of blade: 9 mm
- Thickness of blade: 2 mm
- Contact line pressure: 1.8 g/mm or 2.5 g/mm
- Contact angle: 16°
- Diameter of photoreceptor drum: 100 mm
- Photoreceptor: Se alloy (surface roughness of 0.11 mm or mirror-quality surface)
- Process speed: 382 mm/sec

Friction and Wear Experiment

The experimental results for the friction coefficient are described. In the case the photoreceptor drum with a mirror-quality surface, torque of the drum was T = 4.0 kg cm. Then the friction force per mm of cleaning blade F (g) is calculated to be 2.37 from 4.0 kg cm × 10 mm × 1000 g = (100 mm/2) × F × 338 mm. Therefore the coefficient of friction μ 1.32 is obtained at the contact line pressure of 1.8 g/mm. In the case of the photoreceptor drum with a rough surface, the coefficient of friction μ = 0.82 is obtained for the torque T = 2.5 kg cm.

It can be considered that the difference between the static and kinetic friction coefficient $(\mu_s - \mu_k)$ in Eq. (29) does not depend on the rebound resilience as discussed before. The incremental friction coefficient $\delta\mu$ is assumed to be related to the mechanical arrangement of the copying machine but does not depend on the rebound resilience. Therefore, with a constant value of l, Eqs. (28) and (29) lead to the following equation:

$$1/S = 1/\alpha l = C_1 - C_2 \ln R \tag{30}$$

The wear characteristics of the cleaning blades were investigated in an accelerated wear experiment. The photoreceptor drum with a mirror-quality surface (coefficient of friction = 1.32) was used, and the contact

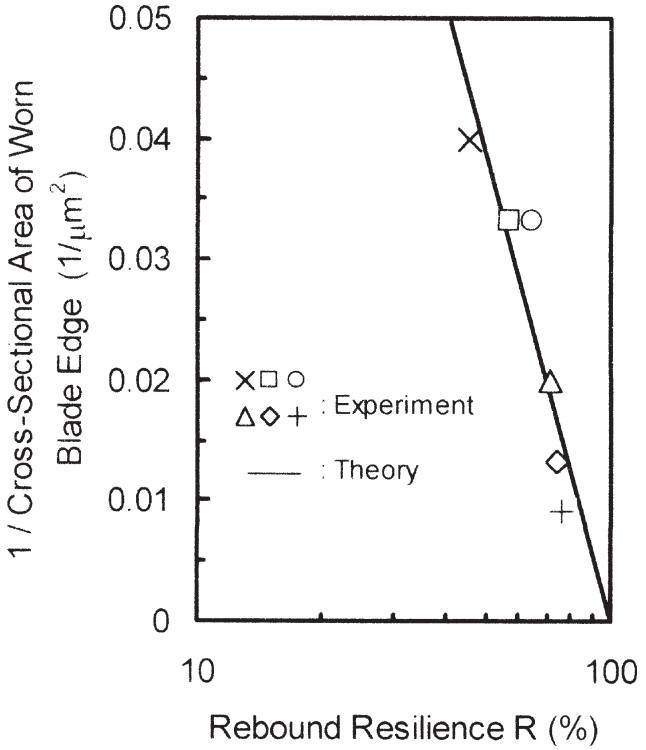

Figure 12. Cross-sectional area of worn blade edges as a function of rebound resilience after 3 hours operation under accelerated wear experiment. Solid line is a least square fit to Eq. (30).

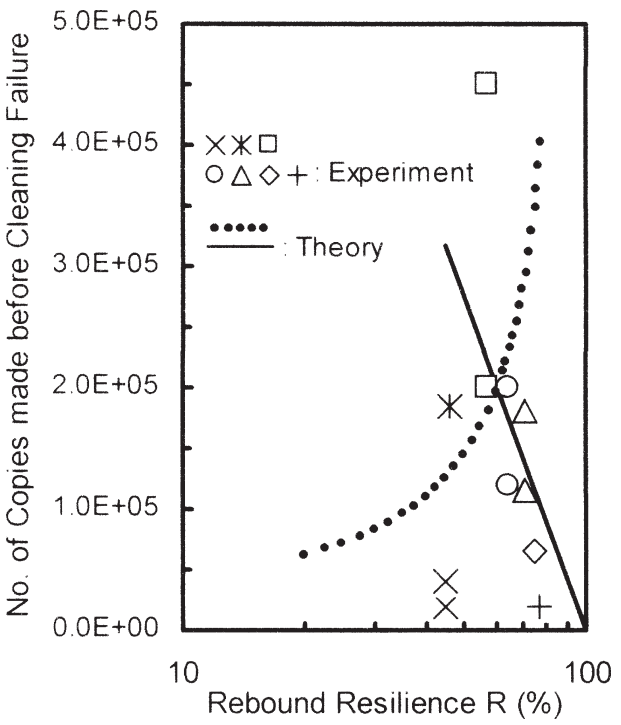

Figure 13. The number of copies made before the cleaning failure as a function of rebound resilience R using 60 cpm copying machines. Solid curve represents the analytical expression, Eq. (39). Dotted curve is the cleaning ability calculated from Eq. (40).

line pressure was increased by 40% up to 2.5 g/mm. Cleaning blade edges were worn for 3 hours (equivalent to the friction length for 10,800 continuous copies) for samples Nos. 1 – 7 as indicated in Table I. The reciprocal of the worn cross-sectional areas of blade edges as a function of the rebound resilience (at 30°C) is shown in Fig. 12. The solid line is obtained by a least squares fit of the experimental data to the simplified form of Eq. (30). The close agreement between the theory and the experimental observation is seen in Fig. 12. C_1 and C_2 are determined to be – 0.0002 μm^{-2} and 0.0556 μm^{-2}, respectively. C_1 can be neglected which means that $L_{sl} >> L_{st}$, namely, the slip distance occupies most of the sliding distance of the cleaning blade on the photoreceptor drum. Therefore, Eq. (30) reduces to the following equation:

$$1/S = -C_2 \ln R = -\left(\frac{C' v \ln R}{L_{hr} \mu^{6.5} W^{3.2}}\right) \tag{31}$$

where C' is a constant, m = 6.5 (in Eq. (29)), L_{hr} is wear time (hours), and v is rotational velocity (m/sec). Substituting v = 0.328 m/sec, μ = 1.32, W = 2.5 g/mm and L_{hr} = 3 h into Eq. (31), we have,

$$C_2 = 9.59 \times 10^{-4} C' = 0.0556 \tag{32}$$

and hence,

$$C' = 58.0 \tag{33}$$

Then the wear equation of our blade cleaning system is obtained as follows:

$$1/S = \frac{58.0 v \ln R}{L_{hr} \mu^{6.5} W^{3.2}} \tag{34}$$

The close agreement between the theory and the experimental observation in Fig. 12 strongly suggests that the wear mechanism of rubber is fatigue destruction.

Cleaning Performance Test

Using three 60 cpm copying machines, the cleaning performance of cleaning blades was evaluated by the number of copies made before a black stripe appeared on a copy. The temperature of the cleaning blade under test was measured as ca. 30°C.

One cycle of copy mode per 24 hours was as follows:
— continuous 1,500 copies
— 1,500 copies made in 6 copy intervals
• Both of these cycles repeated 6 times
— 1,500 copies made in single copy/pause mode.

A total of 16,500 copies were made per 24 hours.

The cleaning performance of samples shown in Table I was evaluated. The relationships between the cleaning performance and hardness, tear strength, 300% modulus and Young's modulus were considered. However, the authors did not find significant correlation with those specifications.

The results of the cleaning performance test, i.e., the relationship between number of copies made before cleaning failure and rebound resilience (at 30°C) is shown in Fig. 13. The peak of the cleaning performance was noted at about R = 50%. Above this value the clean-

ing performance declined as R increased. Below this value the cleaning performance was extremely low.

L_{hr} (hours) during the cleaning performance test is converted into number of copies.

$$L_{hr+} = 24\ N\ /\ 16{,}500 = N/687.5 \tag{35}$$

Then L_{hr} in Eq. (34) is transformed into the number of copies N as follows:

$$\frac{1}{S} = \frac{58.0\,v}{\mu^{6.5} W^{3.2} L_{hr}} \ln R = -\frac{3.99 \times 10^4\, v}{\mu^{6.5} W^{3.2} N} \ln R \tag{36}$$

$$N = -\frac{3.99 \times 10^4\, vS}{\mu^{6.5} W^{3.2}} \ln R \tag{37}$$

The cross-sectional worn area of sample No. 3 with 200,000 copies made before cleaning failure as shown in Fig. 13 was 55 μm². Substituting 55 μm² into S in Eq. (37), we obtain the number of copies made before cleaning failure, N_{life}, of our blade cleaning system as follows:

$$N_{life} = -\frac{2.19 \times 10^6\, v}{\mu^{6.5} W^{3.2}} \ln R \tag{38}$$

With v = 0.328 m/s, μ = 0.82, and W = 1.8 g /mm in Eq. (38), the relationship between N_{life} and rebound resilience R is given by

$$N_{\mathrm{life}} = -\,3.98 \times 10^5 \ln R \tag{39}$$

The line representing the analytical expression, Eq. (39) is indicated in Fig. 13. We infer that cleaning failures may be accidental phenomena caused by e.g., paper dust and impurities. However the analytical solid line does indicate a dependence of the cleaning performance on the rebound resilience.

Cleaning Ability

Cleaning ability was evaluated by the number of copies made before cleaning failure occurred under severe condition for cleaning blades. The 60 cpm copying machine was placed in a 10°C and 15% RH environment. The temperature of the cleaning blades under experiment was measured as about 20°C. A photoreceptor drum with a mirror-quality surface was used. The copy mode was as follows: 100 copies of 6% black and white chart, followed by continuous copies of white chart until cleaning failures occurred. The experimental results are shown in Fig. 14.

Honda observed the behavior of toner particles in the neighborhood of the blade nip through high magnification CCD camera installed inside a transparent glass based organic photoconductor (OPC) drum (transparent to visible light).[6] He observed that toner particles blocked by the cleaning blade accumulate to form a pool of toner. This toner pool is made up of almost immobile toner particles and surface treatment agent particles, that is, a layer slipping with respect to the movement of photoconductive surface. He called this the static toner region. It was found that in the static toner region, the nearer the particles were to the blade edge, the smaller the diameter of toner particles.

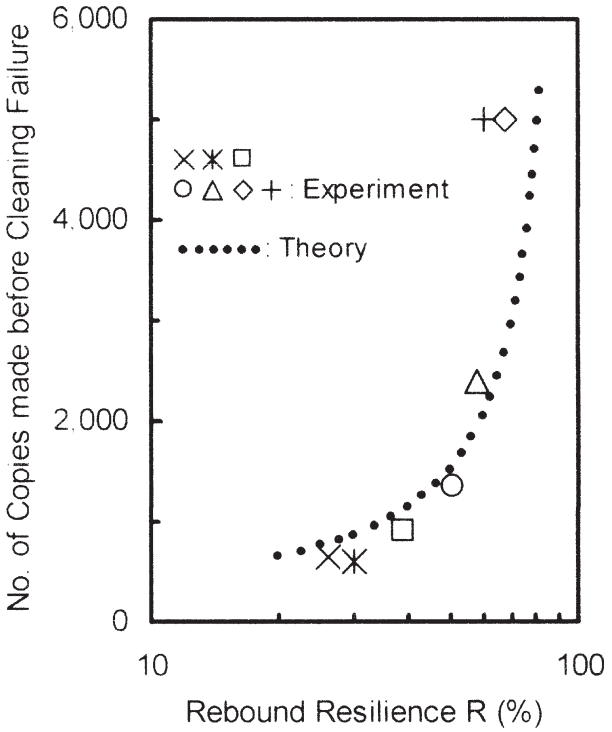

Figure 14. The number of copies made before the cleaning failure as a function of rebound resilience R at 20°C under high load experimental conditions for cleaning blades. Dotted line: cleaning ability calculated from Eq. (40).

The cleaning blade nip and the static toner region move together with the photoreceptor layer during the stick process according to the stick–slip model shown in Fig. 2. Therefore, toner particles cannot pass through the blade nip during the stick process. However, during the slip process, the cleaning blade forces remaining toner particles to move against direction of rotation of the photoreceptor drum. There is thereby a greater possibility of toner particles going through the blade nip during the slip process. Therefore, we think that the cleaning ability is inversely proportional to the slip length as follows:

$$\text{Cleaning ability} \propto 1/L_{\mathrm{sl}} = -\,\mathrm{C}/\ln R \tag{40}$$

This analytical expression is shown in Fig. 14 as a dotted curve. A close agreement between Eq. (40) and the experimental observation is confirmed. When the same dotted curve representing Eq. (40) is inserted in Fig. 13, this model can be applied to explain the reason why the cleaning performance shown in Fig. 13 is extremely low for R below 50%. Both sufficient cleaning ability and reasonable lifetime of cleaning blades are required for practical use. Therefore, sample No. 4 (R = 64% at 30°C) is the optimum choice for our blade cleaning system.

Conclusions

We have examined the general profile of the cleaning performance (cleaning ability and lifetime of cleaning blades) in terms of tribology and rheology. The cleaning performance is found to depend on the stick–slip behavior of the cleaning blade edges. This study has made it

clear that the wear mechanism of the cleaning blades is fatigue destruction, and the cleaning ability strongly depends on the rebound resilience.

Acknowledgment. We would like to express our deepest gratitude for the advice and cooperation of Mr. K. Kubota of Hokushin Corporation, and for the contributions to this study of their colleagues, K. Tange, K. Matsushita, S. Hirota and M. Honda. The authors would also like to thank Dr. Inan Chen for valuable suggestions in the preparation of this article.

References

1. R. J. Meyer, Theory of Blade Cleaning, in *Proc. IS&T's 16th Int'l. Congress on Adv. in Non-Impact Printing Technologies*, IS&T, Springfield, VA, 2000, pp. 846-850.
2. K. Seino, K. Tange, S. Yuge, and M. Uemura, Effect of Rebound Resilience on Blade Cleaning Performance, in *Proc. IS&T's 13th Int'l. Congress on Adv. in Non-Impact Printing Technologies*, IS&T, Springfield, VA, 1997, pp. 59-63.
3. E. Southern and A. G. Thomas, *Plastics and Rubber: Materials and Applications,* 133 (Nov. 1978).
4. Y. Uchiyama and Y. Ishino, *Wear,* 158 (1992)
5. M. Honda and H. Murasaki, *Soc. Electrophot. Jpn.*, **34,** 419 (1995).
6. R. D. Mindlin, *Trans. ASME, Ser. E, J. Appl. Mechanics,* **71,** 259 (1949).
7. *Highpolymer Technology Lectureship 7: Properties and Manufacturing on Rubber*, Chijin-Syokan, Tokyo, p. 302 (in Japanese).